Axial Arrangement of the Myosin Rod in Vertebrate Thick Filaments: Immunoelectron Microscopy with a Monoclonal Antibody to Light Meromyosin

TERUO SHIMIZU, JAMES E. DENNIS, TOMOH MASAKI, and DONALD A. FISCHMAN
Department of Cell Biology and Anatomy, Cornell University Medical College,
New York, New York 10021. Dr. Shimizu's present address is Department of Neurology, Institute of Brain Research, University of Tokyo, 7-3-1-Hongo, Bunkyo-ku, Tokyo, Japan. Dr. Masaki's present address is Department of Pharmacology, Institute of Basic Medical Sciences, The University of Tsukuba, Niihari-Gun, Ibaraki-ken, 305 Japan.

ABSTRACT   A monoclonal antibody, MF20, which has been shown previously to bind the myosin heavy chain of vertebrate striated muscle, has been proven to bind the light mero-myosin (LMM) fragment by solid phase radioimmune assay with alpha-chymotryptic digests of purified myosin. Epitope mapping by electron microscopy of rotary-shadowed, myosin–antibody complexes has localized the antibody binding site to LMM at a point ~92 nm from the C-terminus of the myosin heavy chain. Since this epitope in native thick filaments is accessible to monoclonal antibodies, we used this antibody as a high affinity ligand to analyze the packing of LMM along the backbone of the thick filament. By immunofluorescence microscopy, MF20 was shown to bind along the entire A-band of chicken pectoralis myofibrils, although the epitope accessibility was greater near the ends than at the center of the A-bands. Thin-section, transmission electron microscopy of myofibrils decorated with MF20 revealed 50 regularly spaced, cross-striations in each half A-band, with a repeat distance of ~13 nm. These were numbered consecutively, 1–50, from the A-band to the last stripe, ~68 nm from the filament tips. These same striations could be visualized by negative staining of native thick filaments labeled with MF20. All 50 striations were of a consecutive, uninterrupted repeat which approximated the 14–15-nm axial translation of cross-bridges. Each half M-region contained five MF20 striations (~13 nm apart) with a distance between stripes 1 and 1', on each half of the bare zone, of ~18 nm. This is compatible with a packing model with full, antiparallel overlap of the myosin rods in the bare zone region. Differences in the spacings measured with negatively stained myofilaments and thin-sectioned myofibrils have been shown to arise from specimen shrinkage in the fixed and embedded preparations.

These observations provide strong support for Huxley's original proposal for myosin packing in thick filaments of vertebrate muscle (Huxley, H. E., 1963, J. Mol. Biol., 7:281–308) and, for the first time, directly demonstrate that the 14–15-nm axial translation of LMM in the thick filament backbone corresponds to the cross-bridge repeat detected with x-ray diffraction of living muscle.

The thick myofilaments of vertebrate skeletal muscle are complex polymeric structures composed predominantly of myosin but also contain a set of minor proteins including M-protein (32, 50), C-protein (34, 40), myomesin (16), M-crea-tine kinase (51), H-protein (6), AMP deaminase (1), end-protein (49), and titin or connectin (31, 54).

A basic model for the structure of thick filaments was first described by H. E. Huxley (22). Based on electron microscopy

of single myosin molecules and native and synthetic filaments, he concluded that (a) the globular portion of myosin molecules form projections (cross-bridges) that arise from the filament backbone; (b) the filament backbone is composed of the rod portion of the myosin molecules assembled in a parallel, staggered array; (c) each filament is bipolar, having a region (the bare zone) where myosin rods are in antiparallel orientation; and (d) cross-bridges occur along the length of the thick filament, excluding the bare-zone, and filaments taper at their tips.

x-ray diffraction of living muscle (24) revealed a helical arrangement of the cross-bridges with an axial repeat of 42.9 nm and an axial translation of 14.3 nm. However, since x-ray diffraction only reveals average values for the predominantly repetitive structures, and cross-bridge orientation is quite varied in vivo (13, 24), the precise surface lattice of the cross-bridges has remained a point of dispute until recently (25, 26, 28).

Early electron microscopic studies suggested an axial repeat of ~40 nm in the A-band (10, 21, 35), but precise measurements of the axial repeats were inadequate with conventional analyses of thin sections or with negatively stained, native thick filaments. The first significant details of A-band axial repeats were obtained by O'Brien et al. (33) and Hanson et al. (18), using negatively stained A-segments, which revealed 10 transverse stripes ~42 nm apart in each half A-band, and a poorly resolved set of finer striations in the cross-bridge region. Extending this work, Craig (5) clearly demonstrated eleven transverse bands with a 43-nm repeat and a fine set of 14.3-nm striations in the cross-bridge region. Applying a new approach, negative staining of cryosections of human tibialis muscle, Sjostrom and Squire (45) mapped forty-nine 14.3-nm and eleven 43-nm repeats in each half A-band. However, since many of these repeats could have arisen from non-myosin A-band proteins, it has been difficult to establish their origin with a strictly morphological approach.

Immunoelectron microscopy has been very useful in establishing the distribution of C-protein (7, 9, 40) and M-creatine kinase (53), and will undoubtedly be helpful in localizing other proteins in the thick filament. To date, polyclonal antibodies to myosin (41), myosin subfragment-1 (S1)[1] (8), and the myosin light chains (44) have not been especially helpful in clarifying the cross-bridge surface lattice or the packing of myosin rods within thick filaments.

We now present evidence that a monoclonal antibody (McAb) to light meromyosin (LMM) defines an axial repeat within the A-bands and isolated thick filaments of chicken pectoralis muscle. We suggest that this labeling pattern reflects the axial distribution of the myosin rod along the thick filament and can be used to validate models of myosin packing derived from cross-bridge analysis (5, 8, 36, 37, 46). A preliminary report of this work has been presented (43).

MATERIALS AND METHODS

Myosin from adult chicken pectoralis major muscle was prepared as described previously (2). Digestion with alpha-chymotrypsin was performed by the method of Weeds and Pope (55). Aliquots of the preparation were analyzed by indirect solid phase radioimmune assay (RIA) to establish reactivity with McAb MF20 after proteolytic digestion. After a threefold dilution with distilled water, the myosin digests were dialyzed overnight against LSB (0.04 M NaCl, 10 mM

---

[1] *Abbreviations used in this paper:* FITC, fluorescein isothiocyanate; LMM, light meromyosin; McAb, monoclonal antibody; RIA, radioimmune assay; S1, subfragment-1; S2, subfragment-2.

sodium phosphate, pH 6.4, 1 mM dithiothreitol, 0.1 mM phenylmethylsulfonyl fluoride, and 0.01% sodium azide). Insoluble material containing myosin and LMM was separated from soluble fragments of heavy meromyosin by centrifugation at 40,000 g for 1 h.

Solid Phase RIA

The reactivity of McAb MF20 with unfractionated myosin digests, low salt soluble and insoluble fractions, and purified myosin was assayed by solid phase indirect RIA as previously described (2, 42).

Purification and Labeling of Antibody MF20

The McAb (MF20) used in these experiments was secreted by a mouse-mouse hybridoma and is an IgG1 as determined by the double diffusion method of Ouchterlony (34a; results not shown). The antibody was concentrated and purified as previously described (9). For fluorescein isothiocyanate (FITC) labeling, the antibody (bound to a myosin–Sepharose 4B column) was reacted with 1 mg/ml FITC overnight in 50 mM sodium bicarbonate, pH 7.3 at 4°C. After washing the column in 0.15 M NaCl, 50 mM Tris HCl, pH 7.5, the FITC-labeled antibody was eluted with 0.2 M glycine HCl, pH 2.3. The eluate was dialyzed and stored in solution A (0.1 M KCl, 10 mM MgCl$_2$, 2 mM EGTA, 0.5 mM dithiothreitol, 0.1 mM phenylmethylsulfonyl fluoride, 0.1% sodium azide, 5 mM sodium phosphate, pH 7.0). Unlabeled, purified antibody was dialyzed against the buffers listed below for the following experiments: (a) platinum shadowing of myosin molecules, 0.5 M ammonium formate, pH 6.7; (b) decoration of myofibrils, solution A; and (c) decoration of native thick filaments, solution A + 5 mM ATP.

Iodination of goat anti–mouse IgG was performed while adsorbed to an affinity column of mouse IgG–Sepharose 4B (2).

Preparation of Myofibrils and Myofilaments

Fascicles from adult white Leghorn chickens were prepared as described previously (9).

Myofibrils were prepared by homogenization of the Triton-extracted fiber bundles in 30 ml of solution A in a Sorvall Omni-mixer (DuPont Co., Sorvall Biomedical Division, Newtown, CT) at setting 8 for 30 s. The homogenate was spun at 600 g for 5 min, the supernatant discarded, and the pellet washed five times with solution A, treated 30 min with solution A plus 0.5% Triton X-100, and washed three more times with solution A.

To prepare native myofilaments, the extracted muscle strips were homogenized in 30 ml of solution A containing 10 mM ATP with the same Omni-mixer but at setting 10 for 10–15 s. The homogenate was filtered through four layers of washed cotton cheesecloth and centrifuged at 12,000 g for 1 h. The supernatant was diluted in solution A to a final protein concentration of 0.04 mg/ml.

Immunofluorescent Labeling of Myofibrils with MF20

Direct immunofluorescent labeling was performed at 4°C with myofibrils adherent to glass microscope slides. Some myofibrils were fixed with absolute ethanol or acetone by immersion of the slides for 15 min at 4°C. After flooding the slides in solution A plus 1% bovine serum albumin (BSA) for 5 min, the myofibrils were reacted with FITC-labeled MF20 for varying lengths of time (15 min–12 h). As a control, the myofibrils were incubated in nonimmune mouse IgG (Cappel Laboratories Cochranville, PA) followed by FITC-labeled goat anti–mouse IgG. All slides were washed in solution A, fixed in 4% formaldehyde in phosphate-buffered saline (PBS) for 15 min, and mounted in solution A. Specimens were viewed with Zeiss epifluorescent or phase optics (Carl Zeiss, Inc., Thornwood, NY) using a 100× planapochromatic objective lens under oil immersion. Photomicrographs were taken with Kodak Tri-X film.

Immunoelectron Microscopy

Rotary shadowing of myosin–antibody complexes was performed by the mica replica technique of Hall (17) as modified by Tyler and Branton (52), and was recently used for studies of myosin by Winkelman and Lowey (56, 57). Column purified myosin (0.04 mg/ml) was incubated with affinity purified MF20 (0.04 mg/ml) in 0.5 M ammonium formate buffer (pH 6.7) overnight at 4°C. The antibody–myosin mixture was diluted 1:1 with 60% glycerol in 0.6 M ammonium formate (pH 6.7), sprayed onto freshly cleaved mica, and placed in an Edwards vacuum evaporator (Edwards High Vacuum, Inc., Grand Island,

NY). Specimens were evacuated for 3 h at room temperature (10^{-6} torr), then rotary-shadowed with platinum at an angle of 6° (10 cm distance, 1 cm height), and vertically coated with a thin layer of carbon. The specimens were then removed from the shadow caster, floated onto glass distilled water, and picked up with 400-mesh copper grids.

For labeling of myofibers, strips of Triton-permeabilized muscle were cut and teased into bundles of ~10 × 1 mm and divided into two groups: (a) Ethanol-pretreated muscle. Myofibers were incubated sequentially in 30, 60, 90, and 100% ethanol for 15 min each, and then re-equilibrated in solution A. (b) Native muscle. Myofibers were washed for equivalent lengths of time in solution A at 4°C. Both groups were then treated identically by sequential immersion in solution A plus 1% BSA (1 h) followed by overnight incubation in nonimmune mouse IgG or McAb MF20 (0.2 mg/ml), both in solution A. Specimens were then washed five times in solution A, fixed in 2% glutaraldehyde in PBS (overnight at 4°C), rinsed in 0.1 M sodium cacodylate buffer (pH 7.0), postfixed in 1% OsO₄ in 0.05 M sodium cacodylate (pH 7.0), dehydrated in ethanol, and embedded in Epon 812. Longitudinal sections (60–70-nm thick) were stained with uranyl acetate and lead citrate.

For negative staining, native myofilaments were mixed with an equal volume of affinity purified MF20 (0.04 mg/ml) and incubated overnight at 4°C in solution A containing 5 mM ATP. One drop of this solution was applied to a carbon-coated grid for 15 s, blotted, rinsed quickly with 0.1 M ammonium acetate, pH 6.8, and negatively stained with 1% uranyl acetate, pH 4.3.

All electron microscopy was performed with a JEOL 100 CX-II (JEOL USA, Peabody, MA), operated at 80 kV. Bovine liver catalase crystals (Sigma Chemical Co., St. Louis, MO) and tobacco mosaic virus were used as calibration standards (3, 58). Selected micrographs were used for optical diffraction analysis in the laboratory of Dr. P. Ross Smith, Department of Cell Biology, New York University School of Medicine.

RESULTS

Alpha-Chymotryptic Myosin Digests

Solid phase RIAs were performed with chicken pectoralis myosin after alpha-chymotryptic digestion in high salt. Under these digestion conditions, the MF20 epitope was not destroyed, and all binding activity was recovered in the LMM fraction. Immunoblots of digested myosin showed that the rod, LMM, and shorter tail fragments were reactive with MF20. No antibody binding was detected with purified S1 or subfragment-2 (S2) preparations (results not shown). Thus, the epitope for MF20 resides in the LMM fragment of the myosin rod.

Rotary Shadowing of Antibody–Myosin Complexes

At molar ratios of 1:1 (myosin/McAb), ~75% of the myosin molecules exhibited bound antibody (Fig. 1). 20% of the molecules were unassociated with antibody, and 4% were in large aggregates. Less than 1% of the myosin molecules were decorated with antibody at other sites, which we presume to be nonspecific protein interactions. Measurements were performed to carefully map the MF20 epitope. Rod length was found to be 160 ± 5 nm ($n = 141$),[2] the distance from the carboxy terminal to the hinge region was 166 ± 4 nm ($n = 24$), and the MF20 binding site was placed 92 ± 5 nm ($n = 141$) from the C-terminus or 24 nm from the hinge (Fig. 7). These results confirm and extend the RIA and immunoblot experiments demonstrating epitope localization within LMM.

Immunofluorescent Staining of Myofibrils

Direct immunofluorescent staining of myofibrils with FITC-conjugated MF20 was used to visualize the distribution of MF20 binding sites within the sarcomere (Fig. 2). Different

[2] All measurements are presented as the mean ± one standard deviation; the number of molecules analyzed (n) is presented in parentheses.

A-band staining patterns were observed depending upon the fixation or time of incubation in the McAb. When unfixed myofibrils were incubated in MF20 for up to 20 h at 4°C, staining was predominant at the outer edges of the A-band. Faint reactivity was sometimes observed at the vicinity of the M-band (Fig. 2, a and b). After overnight incubations, most of the A-band stained strongly; the M-band staining remained weak (Fig. 2, c and d). When myofibrils were prefixed in either 100% ethanol or acetone, the labeling patterns for up to 8 h of incubation were similar to those obtained with unfixed specimens, but fluorescence intensity was enhanced with the fixed material (Fig. 2, e and f). Uniform staining of the entire A-band was seen after incubation of fixed myofibrils in MF20 for 18–20 h (Fig. 2, g and h). Sarcomere lengths of fibrils a, b, e, and f were measured, and these were: a, 2.3 μm; b, 1.8 μm; e, 2.5 μm; f, 1.9 μm. There was no correlation of sarcomere length with either the pattern or intensity of MF20 staining. No fluorescence was observed in control samples labeled with FITC-labeled secondary antibody. Also, although the M-band did label in the short antibody incubations, particularly after fixation, we found no evidence for cross-reactivity of MF20 with M-line proteins in our electron microscopy experiments (see below) or immunoblots (2, 15). We conclude that MF20 binds along the entire A-band, and that the observed variations in labeling reflect differences in myosin epitope accessibility within the thick myofilaments.

Thin-Section Immunoelectron Microscopy

Native or ethanol-fixed myofiber bundles were incubated overnight in MF20 or in nonimmune mouse IgG as a control (Fig. 3). In the latter samples, striations were observed in the cross-bridge region of the A-bands, with an axial repeat of 12.8 ± 0.4 nm ($n = 16$). These values were established by optical diffraction of electron micrographs masked to include only the cross-bridge region (Table I).

Additionally, three to five striations were observed in the M-region; these have been described by others (27, 36, 37, 45) and presumably arise from nonmyosin M-band proteins, including M-protein, myomesin, and M-creatine kinase. The precise number of M-region striations varied depending upon the plane of section but averaged five in the best aligned material. Another repeat of ~40 nm could be detected in the cross-bridge region, possibly arising from C-protein. After unfixed myofibrils were decorated with MF20, there was an increased electron density over the entire A-band and the
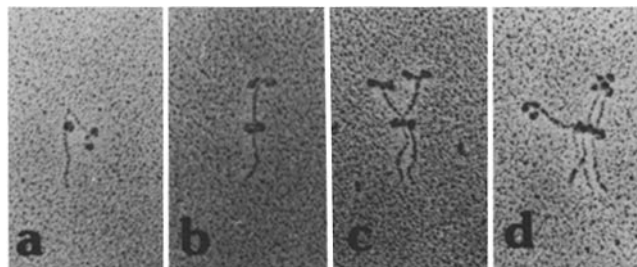

Figure 1 Myosin–antibody (MF20) complexes were visualized by platinum rotary shadowing. Different myosin–antibody complexes were observed. The most abundant form was a dimer (c) which was 48% of the total ($n = 1545$) observed. Monomer forms constituted 19% of the total and were labeled with one (a) or two (b) IgG molecules (14 and 5%, respectively). Trimer forms were 7% (d), and 6% were polymeric forms. × 92,000.
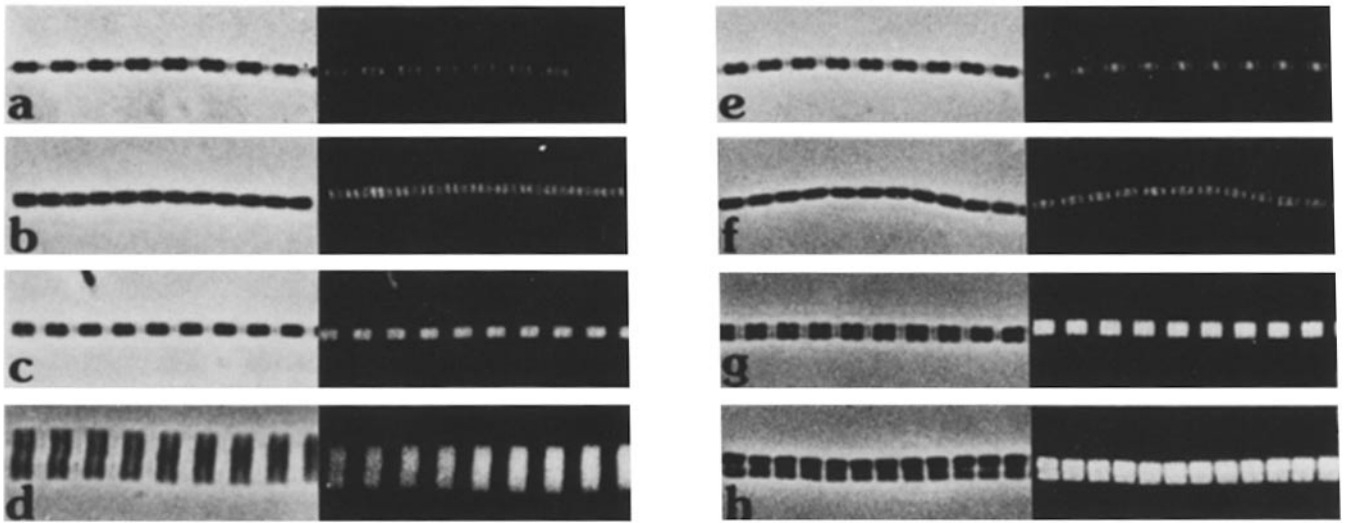
FIGURE 2 Myofibrils with (e–h) or without (a–d) prefixation in ethanol were incubated at 4°C with FITC-labeled MF20. The concentration of IgG was 30 μg/ml in experiments a–c and e–h or 90 μg/ml in d. Phase contrast images are shown to the left of the same fields photographed under fluorescent optics. Samples a, b, e, and f were incubated in FITC-MF20 for 15 min, and those in c, d, g, and h were incubated overnight.
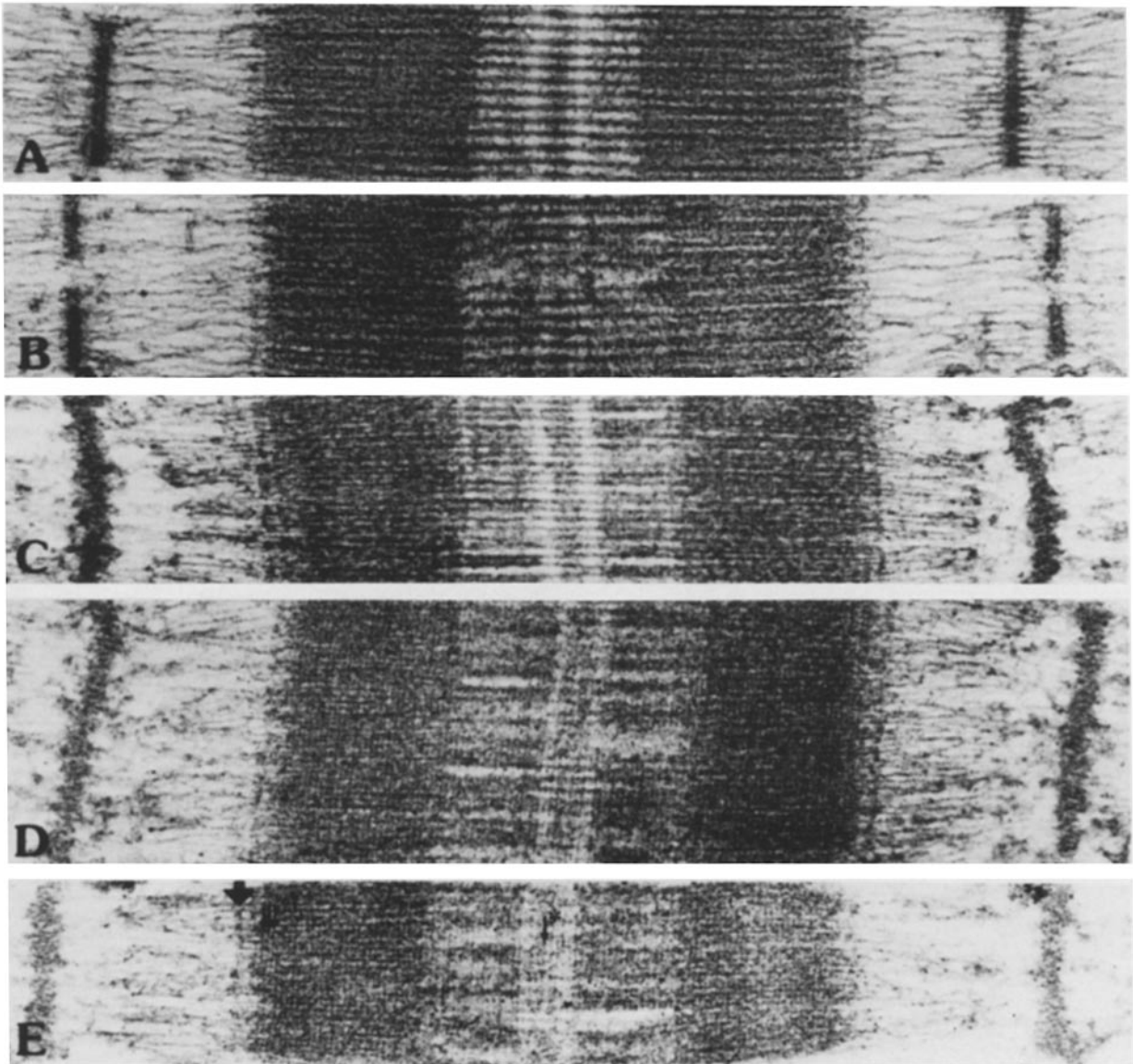
TABLE I. *Periodicity of MF20 Labeling Measured by Optical Diffraction**

	n	First order	Second order	Origin
Without prior fixation				
Control (8 sarcomeres)				
Cross-bridge region	16	12.8 ± 0.4 (12/16)	—	Cross-bridge
Experimental (8 sarcomeres)				
C-zone	16	—	—	
With prior fixation				
Control (7 sarcomeres)				
C-zone	14	12.7 ± 0.7 (12/14)	—	Cross-bridge
M + P	14	—	—	
Total M	7	—	—	
Experimental (8 sarcomeres)				
C-zone	16	12.2 ± 0.4 (16/16)	6.1 ± 0.2 (5/16)	MF20 stripes
M + P	16	12.5 ± 0.4 (16/16)	6.2 ± 0.2 (3/16)	MF20 stripes
Total M	8	13.4 ± 0.5 (8/8)	—	MF20 stripes
		11.8 ± 0.4 (6/8)	—	MF20 stripes

* Average ± SD nm. C-zone, C-protein zone. M + P, half of the M-region plus proximal zone (12 striations). Total M, total M-region. In parentheses, the number of positive sarcomeres/total analyzed sarcomeres is shown.

suggestion of a 13–14-nm repeat in the cross-bridge region (Fig. 3 *B*). However, optical diffraction of these samples failed to reveal any reproducible periodicities in any region of the A-band. After ethanol fixation and incubation in nonimmune IgG, the myofibrils exhibited a significant loss of electron density in the M- and C-regions, and a marginal decline of density in the remainder of A-band (Fig. 3 *C*). After this treatment, the M-stripes and the 40-nm repeat in the cross-bridge region were not well-preserved, but reflections of 12.7 ± 0.7 nm ($n = 12$, Table I) were detected by optical diffraction.

Most revealing, however, were the ethanol-fixed fibers which were then incubated in MF20 (Fig. 3, *D* and *E*). In these sarcomeres, regularly arrayed, transverse striations were obvious along the entire A-band. Of 99 different sarcomeres that were analyzed, we observed that antibody labeling was not always consistent within a single fiber, or even along the same myofibril. We selected eight sarcomeres that exhibited the most complete labeling, and two fields are presented in Fig. 3, *D* and *E*. Photographic enhancement of these repeats by transverse shifts of the photographic paper during printing (20) and their comparison with control muscle fibers is demonstrated in Fig. 4. Identical repeats were observed in both control and experimental preparations; however, the electron density and width of each stripe was enhanced appreciably in the fibers exposed to MF20. We conclude that the antibody is decorating a repetitive structure intrinsic to the A-band. These images exhibited a maximum of 50 continuous, regular striations that were numbered 1–50, from the M-region to the lateral ends of the A-band. Labeling ended at the 50th stripe, 60.0 ± 3.4 nm from the thick filament tips. Striations 50–6 were in the cross-bridge region, 5–1 in the M-region. Stripes 4 and 48 were often weak or poorly resolved (Fig. 4 *C*), but in some sarcomeres the 48th stripe was clearly labeled (left end of Fig. 5 *B*, right ends of Fig. 4, *A* and *B*). From these data, we conclude that all 50 positions contain at least one MF20 binding site, but epitope number or accessibility may differ at some locations.

Optical diffraction analysis was performed by generating scattering diagrams from the M-, P-, and C-zones of A-band halves (47), which are summarized in Table I. No significant differences in the labeling periodicities were detected between the C-zone and the M- plus P-zones (stripes 1–12). Visual analysis of electron micrographs (Figs. 3 *E* and 4 *A–D*) indicated that the distance between the first stripes in each half A-band (1–1') was larger than were the spacings between other stripes. Direct measurements showed that the distance between stripes 1–6 was 13.1 ± 1.3 nm ($n = 16$), while the distance between stripes 1 and 1' was 15.6 ± 1.6 nm ($n = 8$).

Negative Staining of Native Thick Filaments

Control, native thick filaments (Fig. 5 *A*) had well-preserved structural details such as a clear bare zone, lateral projections in the cross-bridge region, and tapered filament tips. When labeled with MF20, the filaments often aligned or aggregated in parallel, and transverse striations were evident (Fig. 5 *B*). No oblique stripes were ever seen. Significant distortion of the MF20-labeled filaments was observed; thick filaments were angulated or S-shaped, bare zones were difficult to distinguish from the cross-bridge regions, and filament tips were frayed or broken. Microcomparitor measurements of the electron micrographs showed a unit repeat of 14.6 ± 1.2 nm based on the analysis of 1,129 stripes along 51 filaments. The total number of stripes along each filament was difficult to measure with assurance because the filaments were often broken and not all stripes were decorated on each filament. Furthermore, the density of the different positions varied. Two out of 51 filaments were well-preserved along the whole length and, in these, the labeling repeat was 15.2 ± 0.4 nm in the cross-bridge region and 15.3 ± 0.4 nm in M- plus P-zones (stripes 1–12). The distance between stripes 1 and 1' of these two thick filaments was 15.5 and 16.6 nm, which again suggests that the 1–1' spacing is greater than that between other adjacent stripes of the A-band.

FIGURE 3   Electron microscopy of thin sectioned, permeabilized muscle bundles labeled wth MF20. The fibers in *A* and *B* were unfixed, and those in *C*, *D*, and *E* were prefixed in ethanol before incubation in nonimmune mouse IgG (*A* and *C*) or McAb MF20 (*B*, *D*, and *E*). The transverse stripes were numbered 1–50; the first is indicated (*) at the center of the M-band. The last three stripes are also indicated (↓↓↓) beginning 60-nm medial to the lateral border of the A-band (➡). × 61,000.
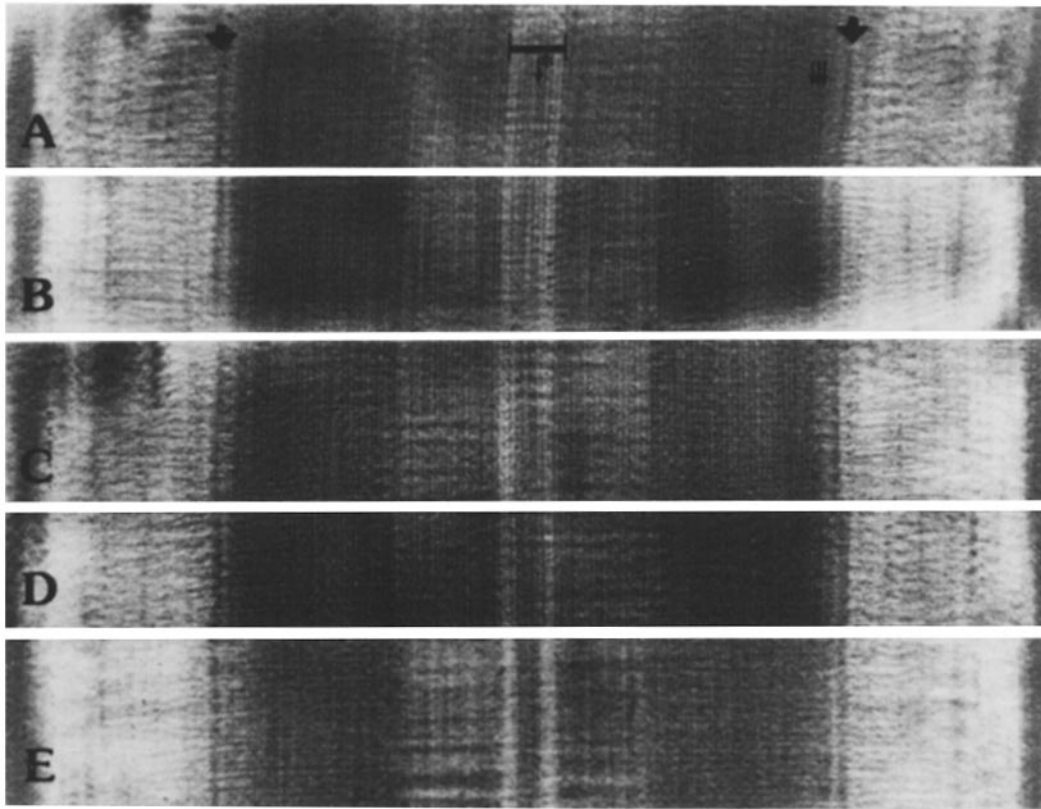
FIGURE 4 Photographic image–averaging of fibers labeled with MF20 (A–D) or incubated in nonimmune mouse IgG (E). All were prefixed in ethanol. In A, the M-region is indicated by brackets and contains four stripes, the first marked (*). ↓↓↓, as in legend to Fig. 3. × 60,000.
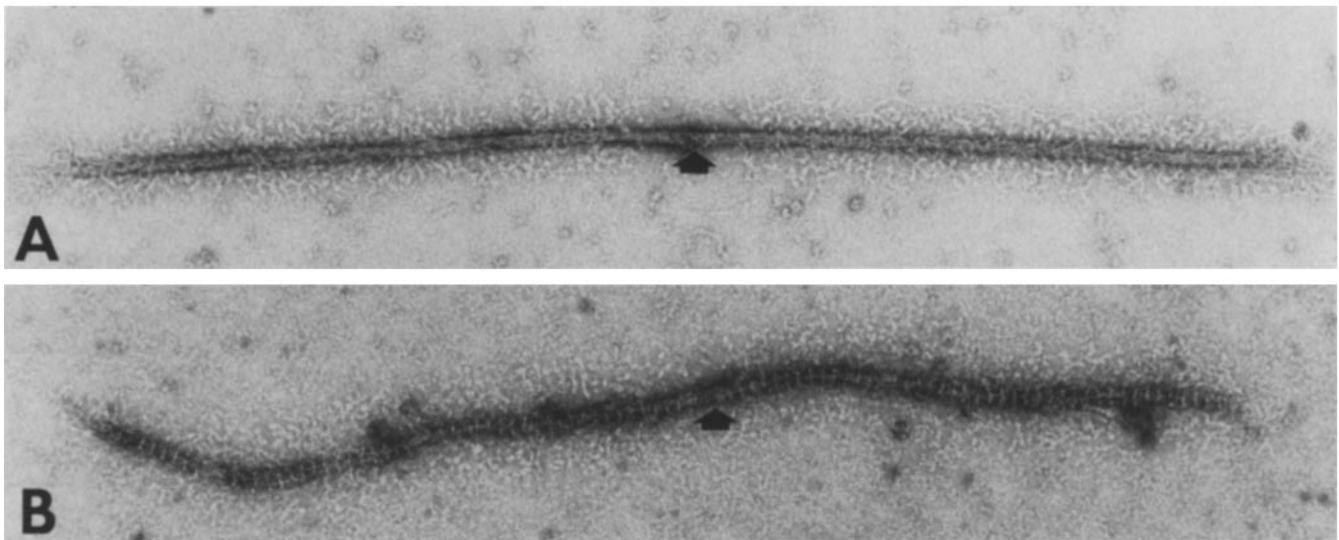

FIGURE 5   Negatively stained native thick filaments after incubation in nonimmune mouse IgG or McAb MF20. × 110,000.

DISCUSSION

Based on these experiments, we conclude that: (a) McAb MF20 binds to an epitope located 92 nm from the C-terminus of MHC; (b) this antibody binds to thick filaments at 50 regularly spaced sites in each half A-band; (c) the accessibility of MF20 for its epitope varies along the length of the filament and this may reflect differences in LMM packing near the filament surface; (d) the unit spacing was ~13 nm in ethanol-fixed, Epon-embedded material and 14.5 nm in negatively stained thick filaments; (e) the different values in negatively stained and thin-sectioned material result from an ~14% shrinkage in length during ethanol fixation and Epon embedding of the fibrils prepared for microtomy; (f) the 50th stripe is located ~68 nm from the filament tip (when corrected for shrinkage), in good agreement with the measured distance between the epitope and the S1 region of single myosin molecules (68 nm); (g) the distance between the first labeling

positions in each half M-band (stripes 1 and 1') is ~3–4 nm longer than is the spacing between other stripes in the A-band.

Analysis of Single Molecules

Our measurements of myosin molecules by rotary shadowing are in good agreement with those of Elliott and Offer (11, 12). We measured the rod length to be 160 ± 5 nm, and the length of LMM (i.e., distance from the tip of the rod to the sharply bent hinge) to be 116 ± 4 nm; Eliott and Offer's measurements of these same portions of the molecule were 156 ± 5 nm and 111 ± 3 nm, respectively. Earlier estimates of rod length were in the range of 134–152 nm (11, 22, 29). By negative staining, the rod length has been measured to be 145 nm (4, 19, 48). Our measurements of rotary-shadowed myosin–IgG complexes indicate that the epitope for MF20 is located 92 nm from the carboxyl tip of the myosin rod.

Myofibril and Myofilament Labeling Patterns

Direct immunofluorescent labeling of myofibrils with MF20 produced a variety of staining patterns depending upon incubation time in the McAb or prefixation in ethanol or acetone. These results may indicate partial blockade of the epitope by nonmyosin proteins in the A-band and by the molecular packing of myosin within the thick filaments. At short incubation times (15 min), antibody staining was predominantly in the lateral regions of the A-band, whereas longer incubation times (18–24 h) produced an even staining of the entire A-band, except for a narrow zone in the M-band region. These staining patterns differ from those of Pepe (36–39) and more closely resemble those of Lowey and Steiner (30). After absorption of polyclonal anti-myosin with heavy meromyosin, Pepe observed almost exclusive labeling at the lateral ends of the A-bands, regardless of sarcomere length or incubation time. Lowey and Steiner (30) also observed non-uniform fluorescent patterns but indicated that LMM staining could also occur in the nonoverlap region and, to a lesser extent, in regions adjacent to the H-zone. Our results clearly prove that anti-LMM staining can occur along almost the entire length of the A-band. Presumably, MF20 recognizes a region of LMM that was only weakly detected by the antibody preparations of Pepe and, possibly, Lowey and Steiner. Antibodies to myosin S2 (30, 39) produce a staining pattern that is similar to that produced when unfixed myofibrils are incubated in MF20 for 18 h. Our results would suggest that myosin S1, S2, and at least the rostral 60–70 nm of LMM are exposed along the thick filament shaft. In this regard, an antibody to the caudal end of LMM (57) would be interesting to apply in further labeling studies.

Ethanol pretreatment of the myofibrils enhanced the fluorescent labeling intensity of FITC-MF20 and substantially improved transmission electron microscopic visualization of the transverse striations in the M-region (M-band plus bare zone) in embedded material. However, ethanol prefixation was not required for decoration of the M-region of isolated native filaments. We can only speculate that ethanol disrupted C-protein binding and M-bridge structure since a 40-nm repeat (interpreted as the C-protein periodicity) was lost, and M-band density significantly reduced, after ethanol treatment of the fibrils. Perhaps, extraction and/or disruption of these elements, or distortion of the LMM packing, permitted better antibody penetration of the A-bands and labeling of the

filaments.

In ethanol-fixed muscle fiber bundles, MF20 labeling produced 50 transverse striations in each half A-band, including the M-region. The periodicity was identical to that seen in the cross-bridge region of unlabeled muscle, with or without ethanol prefixation. Since the latter repeat is interpreted to arise from the cross-bridges at 14.3 nm (21, 22, 24, 45), the antigenic sites are axially translated by a similar repeat in vivo. This is also supported by our negatively stained images of MF20-decorated thick filaments.

We are convinced that our results indicate the axial translation of LMM and not the cross-bridge repeat for the following reasons: (a) control specimens did not exhibit a clear 14–15-nm periodicity along the full length of the A-band; (b) after MF20 labeling, the repeat was seen in the M-band and bare zone regions that lack cross-bridges; and (c) after negative staining, the cross-bridges were not well-resolved in isolated thick filaments, yet the antibody stripes were obvious along the whole shaft of these filaments.

We are also certain that the labeling pattern observed in the M-band did not arise from M-band proteins since ethanol-prefixed muscle lacked the characteristic M-band striations, and isolated thick filaments often lack M-protein (14), yet decorate strongly with MF20.

Implications for Myosin Packing in Thick Filaments

A number of models for the axial arrangement of myosin have been described that were derived from electron microscopy of cross-bridge periodicities (Fig. 6). Craig (5) followed up the work of Hanson et al. (18) on negatively stained A-segments, and was able to demonstrate transverse, stain-excluding stripes ~14.3-nm apart and 7.0-nm wide throughout most of the A-band. No periodicity was detected in the M-band region, and a single gap in the periodic array was reported between the second and third rows medial to the filament tips (Fig. 6C). Sjostrom and Squire (45), using negatively stained cryosections from human anterior tibialis muscle, demonstrated stain-excluding stripes along the entire length of the A-band including part of the M-region. 49 stripes with a repeat distance of 14–15 nm were detected in the cross-bridge region, with one repeat having no stripe between the second and third stripes, moving medially from the filament tips. Seven of these stain-excluding stripes were interpreted to arise from myosin rod and not from cross-bridges (Fig. 6B).
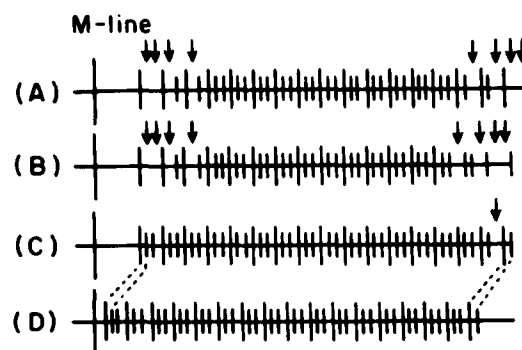

Figure 6 Schematic diagrams of the proposed arrangement of cross-bridge (A–C) and MF20 periodicities (D) according to Squire (46) (A), Sjostrom and Squire (45) (B), Craig and Offer (7) (C), and the present study (D). Arrows indicate the suspected missing rows of cross-bridges.

Using data obtained by Hanson et al. (18), Squire (46) postulated that there were four missing rows of cross-bridges at the proximal and distal portions of the cross-bridge region (Fig. 6, A and B).

Antibody labeling of S1 has been used by Craig and Offer (8) and Pepe (41) to define the axial cross-bridge distribution. They demonstrated the presence of bound antibody along the whole A-band except for the M-region and a small gap near the filament tip. However, no periodic cross-bridge repeats could be defined with their antibody preparations. In Pepe's original model (36, 38), no cross-bridge gaps were suggested in the axial 14.3-nm repeat. Later, he also observed a gap near the filament tip in muscle labeled with polyclonal antibodies to myosin and proposed a similar axial distribution of cross-bridges to that suggested by Craig and Offer (8).

Our own results fit best with the model proposed by Craig and Offer (8), but since our McAb reacts with the rod, we can make no comment about the presence or absence of cross-bridges corresponding to each 14.3-nm LMM repeat. Although we did not find any consistent gaps in the 14–15-nm repeat after labeling with MF20, stripe 48 was often less intensely labeled, and this may correspond to the cross-bridge gap near the filament tips first observed by Craig and Offer (8). Thus, our results indicate an uninterrupted axial spacing of myosin rods in the C-protein zone, proximal (P) zone, and M-regions, in agreement with the conclusions of Sjostrom and Squire (45).

Assuming 14% shrinkage in our ethanol prefixed and embedded bundles, then the 50th MF20 binding stripe was located 68 nm from the filament tip, which corresponds to the last row of cross-bridges. These measurements are consistent with our results on labeled molecules that show the MF20 binding site located 68 nm from the myosin head region.

Antiparallel Packing in the M-region

Previous models for the antiparallel packing of myosin molecules in the bare zone were derived from measurements of bare zone width, i. e., the distance between the first row of cross-bridges in each half A-band, and from measurements of myosin molecular length. Estimates of this width have been obtained with isolated thick filaments: 150–200 nm (22), 120–150 nm (23), 170 nm (46), from thin-sectioned muscle: 154 nm (8), 162 nm (45), from negatively stained A-segments: 149 nm (5). Pepe (36, 38) suggested a 55% antiparallel rod overlap of 86 nm (a bare zone of 200 nm), while Harrison et al. (19) estimated 83% rod overlap or 130 nm (a bare zone of 160 nm).

Based on measurements of the distance between the first MF20 stripes in each A-band half and epitope localization along single myosin molecules, we have estimated the antiparallel overlap of myosin molecules in the M-band region. The distance between stripes 1 and 1' was 15.6 ± 1.6 nm, as derived from measurements of thin-sectioned specimens. When corrected for shrinkage, this value is 18 nm. A diagram of myosin packing is presented in Fig. 7, which positions the MF20 epitopes of the first two myosin molecules 18-nm apart. In this arrangement, the myosin rods are completely overlapped, and the C-terminal portion of one rod may even extend past the N-terminal portion of an opposing molecule. In addition, this model would predict a bare zone width of 154 nm, identical to the measured value of Craig and Offer (8).
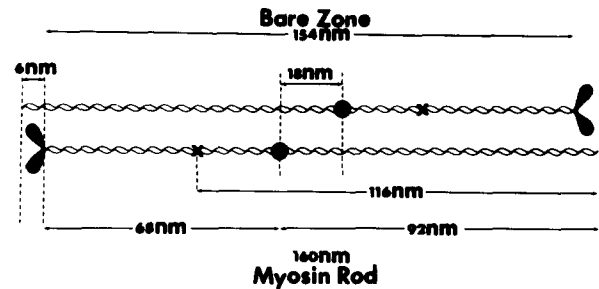

FIGURE 7 Diagram of the maximal overlap of the first two myosin molecules in the middle of vertebrate thick filament. Myosin molecule length and the MF20 binding site (●) were determined from measurements of rotary shadowed molecules. The 18-nm distance between the first two MF20 binding sites was determined from measurements of thin sectioned material. The 154-nm bare zone and the 6-nm figure were derived from measured values. X, hinge region.

REFERENCES

1. Ashby, B., C. Frieden, and R. Bischoff. 1979. Immunofluorescent and histochemical localization of AMP deaminase in skeletal muscle. J. Cell Biol. 81:361-373.
2. Bader, D., T. Masaki, and D. A. Fischman. 1982. Immunochemical analysis of myosin heavy chain during avian myogenesis in vivo and in vitro. J. Cell Biol. 95:763-770.
3. Caspar, D. L. D. 1963. Assembly and stability of the tobacco mosaic virus particle. Adv. Protein Chem. 18:37-122.
4. Cohen, C., S. Lowey, R. G. Harrison, J. Kendrick-Jones, and A. G. Szent-Gyorgyi. 1970. Segments from myosin rods. J. Mol. Biol. 47:605-609.
5. Craig, R. 1977. Structure of A-segments from frog and rabbit skeletal muscle. J. Mol. Biol. 109:69-81.
6. Craig, R., and J. Megerman. 1979. Electron microscope studies on muscle thick filaments. In Motility in Cell Function. F. A. Pepe, J. W. Sanger, and V. T. Nachmias, editors. Academic Press, Inc., New York. 91-102.
7. Craig, R., and G. Offer. 1976. The location of C-protein in rabbit skeletal muscle. Proc. R. Soc. Lond. B Biol. Soc. 192:451-461.
8. Craig, R., and G. Offer. 1976. Axial arrangement of crossbridges in thick filaments of vertebrate skeletal muscle. J. Mol. Biol. 102:325-332.
9. Dennis, J. E., T. Shimizu, F. C. Reinach, and D. A. Fischman. 1984. Localization of C-protein isoforms in chicken skeletal muscle: ultrastructural detection using monoclonal antibodies. J. Cell Biol. 98:1514-1522.
10. Draper, M. H., and A. J. Hodge. 1949. Studies on muscle with the electron microscope. I. The ultrastructure of toad striated muscle. Aust. J. Exp. Biol. Med. Sci. 27:465-503.
11. Elliott, A., G. Offer, and K. Burridge. 1976. Electron microscopy of myosin molecules from muscle and non-muscle sources. Proc. R. Soc. Lond. B Biol. Sci. 193:45-53.
12. Elliott, A., and G. Offer. 1978. Shape and flexibility of the myosin molecule. J. Mol. Biol. 123:505-519.
13. Elliott, G. F., J. Lowy, and B. M. Millman. 1967. Low angle x-ray diffraction studies of living striated muscle during contraction. J. Mol. Biol. 25:31-45.
14. Etlinger, J. D., R. Zak, and D. A. Fischman. 1976. Compositional studies of myofibrils from rabbit striated muscle. J. Cell Biol. 68:123-141.
15. Fischman, D. A., and T. Masaki. 1982. Immunochemical analysis of myosin with monoclonal antibodies. In Perspectives in Differentiation and Hypertrophy. W. Anderson and W. Sadler, editors. Elsevier/North Holland Biomedical Press, Amsterdam. 271-291.
16. Grove, B. K., V. Kurer, C. Lehner, T. C. Doetschman, J.-C. Perriard, and H. M. Eppenberger. 1984. A new 185,000-dalton skeletal muscle protein detected by monoclonal antibodies. J. Cell Biol. 98:518-524.
17. Hall, C. E. 1956. Method for the observation of macromolecules with the electron microscope. Illustrated with micrographs of DNA. J. Biophys. Biochem. Cytol. 2:625-628.
18. Hanson, J., E. J. O'Brien, and P. M. Bennett. 1971. Structure of the myosin-containing filament assembly (A-segment) separated from frog skeletal muscle. J. Mol. Biol. 58:865-871.
19. Harrison, R. G., S. Lowey, and C. Cohen. 1971. Assembly of myosin. J. Mol. Biol. 59:531-535.
20. Horn, R. W., and R. Markham. 1972. Applications of optical diffraction image reconstruction techniques to electron micrographs. In Practical Methods in Electron Microscopy. Volume 1, part 2. A. M. Glauert, editor. Elsevier/North Holland Biomedical

Press, Amsterdam. 327–434.

21. Huxley, H. E. 1957. The double array of filaments in cross-striated muscle. *J. Biophys. Biochem. Cytol.* 3:631–648.

22. Huxley, H. E. 1963. Electron microscope studies on the structure of natural and synthetic protein filaments from striated muscle. *J. Mol. Biol.* 7:281–308.

23. Huxley, H. E. 1964. The fine structure of striated muscle and its functional significance. *Harvey Lect.* 60:85–118.

24. Huxley, H. E., and W. Brown. 1967. The low-angle X-ray diagram of vertebrate striated muscle and its behaviour during contraction and rigor. *J. Mol. Biol.* 30:383–434.

25. Ip, W., and J. Heuser. 1983. Direct visualization of the myosin crossbridge helices on relaxed rabbit psoas thick filaments. *J. Mol. Biol.* 171:105–109.

26. Kensler, R. W., and R. J. C. Levine. 1982. Determination of the handedness of the crossbridge helix of *Limulus* thick filaments. *J. Muscle Res. Cell Motil.* 3:349–361.

27. Knappeis, G. G., and F. Carlsen. 1968. The ultrastructure of the M line in skeletal muscle. *J. Cell Biol.* 38:202–211.

28. Levine, R. J. C., R. W. Kensler, M. C. Reedy, W. Hofmann, and H. A. King. 1983. Structure and paramyosin content of tarantula thick filaments. *J. Cell Biol.* 97:186–195.

29. Lowey, S., H. S. Slayter, A. Weeds, and H. Baker. 1969. Structure of the myosin molecule. I. Subfragments of myosin by enzymic degradation. *J. Mol. Biol.* 42:1–29.

30. Lowey, S., and L. A. Steiner. 1972. An immunochemical approach to the structure of myosin and the thick filament. *J. Mol. Biol.* 65:111–126.

31. Maruyama, K., S. Kimura, K. Ohashi, and Y. Kuwano. 1981. Connectin, an elastic protein of muscle. Identification of "titin" with connectin. *J. Biochem. (Tokyo).* 89:701–709.

32. Masaki, T., and O. Takaiti. 1974. M-protein. *J. Biochem. (Tokyo).* 75:367–380.

33. O'Brien, E. J., P. M. Bennett, and J. Hanson. 1971. Optical diffraction studies of myofibrillar structure. *Philos. Trans. R. Soc. Lond. B Biol. Sci.* 261:201–208.

34. Offer, G., C. S. Moos, and R. Starr. 1973. A new protein of the thick filaments of vertebrate skeletal myofibrils. Extraction, purification and characterization. *J. Mol. Biol.* 74:653–676.

34a. Ouchterlony, O. 1958. Diffusion-in-gel methods of immunological analysis. *Prog. Allergy.* V:1–78.

35. Page, S. G., and H. E. Huxley. 1963. Filament lengths in striated muscle. *J. Cell Biol.* 19:369–390.

36. Pepe, F. A. 1967. The myosin filament. I. Structural organization from antibody staining observed in electron microscopy. *J. Mol. Biol.* 27:203–225.

37. Pepe, F. A. 1967. The myosin filament. II. Interaction between myosin and actin filaments observed using antibody staining in fluorescent and electron microscopy. *J. Mol. Biol.* 27:227–236.

38. Pepe, F. A. 1971. Structure of the myosin filament of striated muscle. *Prog. Biophys. Mol. Biol.* 22:77–96.

39. Pepe, F. A. 1975. Structure of muscle filaments from immunohistochemical and ultrastructural studies. *J. Histochem. Cytochem.* 23:543–562.

40. Pepe, F. A., and B. Drucker. 1975. The myosin filament. III. C-protein. *J. Mol. Biol.* 99:609–617.

41. Pepe, F. A. 1982. The structure of vertebrate skeletal-muscle myosin filaments. *In* Cell and Muscle Motility. Volume 2. R. M. Dowben and J. W. Shay, editors. Plenum Publishing Corp., New York. 141–171.

42. Reinach, F. C., T. Masaki, S. Shafiq, T. Obinata, and D. A. Fischman. 1982. Isoforms of C-protein in adult chicken skeletal muscle: detection with monoclonal antibodies. *J. Cell Biol.* 95:78–84.

43. Shimizu, T., J. E. Dennis, T. Masaki, and D. A. Fischman. 1985. Axial arrangement of the myosin rod in vertebrate thick filaments: immunoelectron microscopy with a monoclonal antibody to light meromyosin. *Biophys. J.* 47(2, Pt. 2):348a.

44. Silberstein, L., and S. Lowey. 1981. Isolation and distribution of myosin isoenzymes in chicken pectoralis muscle. *J. Mol. Biol.* 148:153–189.

45. Sjostrom, M., and J. M. Squire. 1977. Fine structure of the A-band in cryosections. The structure of the A-band of human skeletal muscle fibres from ultra-thin cryosections negatively stained. *J. Mol. Biol.* 109:49–68.

46. Squire, J. M. 1973. General model of myosin filament structure. III. Molecular packing arrangements in myosin filaments. *J. Mol. Biol.* 77:291–323.

47. Squire, J. M. 1981. The Structural Basis of Muscular Contraction. J. M. Squire, editor. Plenum Publishing Corp., New York.

48. Takahashi, K. 1978. Topography of the myosin molecule as visualized by an improved negative staining method. *J. Biochem. (Tokyo).* 83:905–908.

49. Trinick, J. A. 1981. End-filaments: a new structural element of vertebrate skeletal muscle thick filaments. *J. Mol. Biol.* 151:309–314.

50. Trinick, J., and S. Lowey. 1977. M-protein from chicken pectoralis muscle: isolation and characterization. *J. Mol. Biol.* 113:343–368.

51. Turner, D. C., T. Walliman, and H. M. Eppenberger. 1973. A protein that binds specifically to the M-line of skeletal muscle is identified as the muscle form of creatine kinase. *Proc. Natl. Acad. Sci. USA.* 70:702–705.

52. Tyler, J. M., and D. Branton. 1980. Rotary shadowing of extended molecules dried from glycerol. *J. Ultrastruct. Res.* 71:95–102.

53. Wallimann, T., D. C. Turner, and H. M. Eppenberger. 1977. Localization of creatine kinase isoenzymes in myofibrils. I. Chicken skeletal muscle. *J. Cell Biol.* 75:297–317.

54. Wang, K., J. McClure, and A. Tu. 1979. Titin: major myofibrillar components of striated muscle. *Proc. Natl. Acad. Sci. USA.* 76:3698–3702.

55. Weeds, A. G., and B. Pope. 1977. Studies on the chymotryptic digestion of myosin. Effects of divalent cations on proteolytic susceptibility. *J. Mol. Biol.* 111:129–157.

56. Winkelman, D. A., and S. Lowey. 1983. Myosin topography by immuno-electron microscopy using monoclonal antibodies. *Biophys. J.* 41(2, Pt. 2):228a.

57. Winkelman, D. A., S. Lowey, and J. L. Press. 1983. Monoclonal antibodies localize changes on myosin heavy chain isozymes during avian myogenesis. *Cell.* 34:295–306.

58. Wrigley, N. G. 1968. The lattice spacing of crystalline catalase as an internal standard of length in electron microscopy. *J. Ultrastruct. Res.* 24:454–464.